N89-19263

UNSTEADY AERODYNAMICS OF BLADE ROWS

Joseph M. Verdon
United Technologies Research Center
East Hartford, Ct.

PRECEDING PAGE BLANK NOT FILMED

INTRODUCTION

The requirements placed on an unsteady aerodynamic theory intended for turbomachinery aeroelastic or aeroacoustic applications will be discussed along with a brief description of the various theoretical models that are available to address these requirements. The major emphasis is placed on the description of a linearized inviscid theory which fully accounts for the affects of a nonuniform mean or steady flow on unsteady aerodynamic response. Although this linearization has been developed primarily for blade flutter prediction, more general equations will be presented which account for unsteady excitations due to incident external aerodynamic disturbances as well as those due to prescribed blade motions. In this presentation we will focus on the motivation for this linearized unsteady aerodynamic theory, outline its physical and mathematical formulation and present examples to illustrate the status of numerical solution procedures and several effects of mean-flow nonuniformity on unsteady aerodynamic response. This presentation is based on a paper of the same title which is published in full in the Proceedings of the Tenth U. S. National Congress of Applied Mechanics (ref 1).

- **Linearized unsteady aerodynamic analysis**
  - **Real blade geometry**
  - **Mean blade loading**
  - **Shock phenomena**
- **Design applications**
  - **Aeroelastic**
    - **Blade flutter and forced vibration**
  - **Aeroacoustic**
    - **Noise generation, transmission and reflection**

MAJOR ASSUMPTIONS

The development of theoretical models to predict unsteady flows through turbomachines is a formidable task. The analyst is confronted with determining the time-dependent, three-dimensional flow of a viscous compressible fluid through a geometric configuration of enormous complexity. This task has required the introduction of a considerable number of simplifying assumptions to make the problem mathematically tractable and to render the resulting solutions useful to designers. For the most part, the theoretical formulations that have been developed to predict the unsteady aerodynamic phenomena associated with blade flutter or forced vibration consider the blades of an isolated two-dimensional cascade, neglect viscous effects at the outset and regard unsteady fluctuations to be of sufficiently small amplitude so that a linearized treatment of the unsteady perturbation is justified. In addition the resulting two-dimensional inviscid flow is assumed to remain attached to the blade surfaces, the mean flow is assumed to be at most a small irrotational steady perturbation from a uniform stream at the cascade inlet, and any shocks that might occur are assumed to be of weak to moderate strength and have small curvature.

- **Isolated blade row**
- **Two-dimensional inviscid ($Re \rightarrow \infty$) flow**
- **Small-amplitude periodic unsteady excitations**
- **Attached flow**
- **Irrotational mean flow at Inlet:**
  $\vec{V} = \vec{V}_{-\infty} + \nabla\bar{\phi}$
- **Weak shocks**

REQUIREMENTS

In general, the unsteady aerodynamic analyses intended for turbomachinery aeroelastic applications must be applicable to fan, compressor and turbine cascades, to subsonic, transonic and supersonic Mach numbers and to moderate through high frequency structural and external aerodynamic excitations. Then, to determine the aeroelastic and aeroacoustic characteristics of the blading such analyses must be capable of predicting the unsteady loads acting on the blades and the amplitude and wave numbers of the acoustic waves which carry energy away from the blade row and the entropic and vortical fluctuations which are convected downstream. These responses arise from the various sources of unsteady excitation including prescribed blade motions, variations in total temperature and pressure ("entropy and vorticity waves") at inlet, and variations in static pressure (acoustic waves) at inlet and exit. For blade flutter applications it is only necessary to predict the unsteady loads acting on the blades as a result of prescribed blade motions; for forced response applications the unsteady blade loads due to incident entropic, vortical and acoustic disturbances are also required. Finally, for aeroacoustic applications the parameters associated with far-field acoustic responses must be determined.

- **Fan, compressor and turbine cascades**
- **Subsonic, transonic, supersonic Mach numbers**
- **Moderate to high excitation frequencies**
- **Response predictions**
  - **On blades: surface pressures, global unsteady airloads**
  - **Far field: outward propagating acoustic waves vorticity and entropy variations downstream**
- **Prescribed excitations**
  - **Blade motions (flutter)**
  - **External aerodynamic disturbances (forced vibration)**
    - **Vortical and entropic disturbances at inlet**
    - **Acoustic disturbances at inlet and exit**

TRANSONIC CASCADE: $M_\infty < M_{-\infty} < 1$

A representative cascade configuration is shown in the figure below which depicts a two-dimensional section of a transonic compressor rotor ($M_\infty < M_{-\infty} < 1$. The cascade stagger angle is denoted by Θ and the blade spacing by G. In the absence of unsteady excitation the blades are identical in shape, equally spaced and their chord lines are oriented at the same angle, Θ, relative to the axial flow direction. The inlet and exit free-stream flows are described by the velocity vectors $\vec{V}_{\mp\infty}$. The free-stream flow angles measured relative to the axial-flow (or ξ-) direction are denoted by $\Omega_{\mp\infty}$. For the configuration illustrated the inlet and exit conditions are such that normal shocks (Sh) emanate from the blade suction surfaces and vortex wakes (W) emanate from the blade trailing edges and extend downstream.

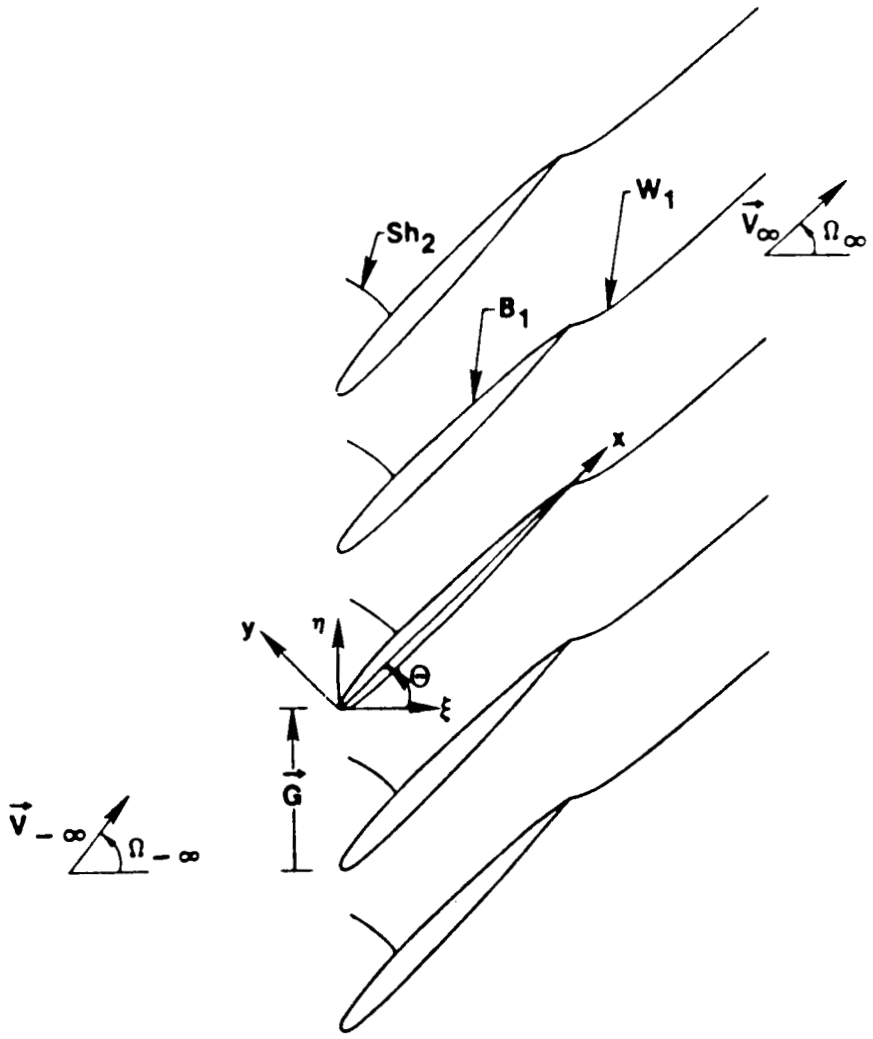

UNSTEADY EXCITATIONS

The unsteady fluctuations in the flow arise from one or more of the following prescribed sources: blade motions, upstream and/or downstream acoustic disturbances which carry energy toward the blade row, and upstream entropic and vortical disturbances which are convected through the blade row by the mean flow. These excitations are assumed to be of small amplitude and periodic in time. The external aerodynamic excitations are also spatially periodic, while the structural excitation is periodic in the "circumferential" or η-direction. For example, we consider blade motions and incident acoustic disturbances as described below. Here $\vec{\mathcal{R}}$ measures the displacement of a point on a moving blade surface relative to its mean or steady-state position, $\vec{X}$ is a position vector, m is a blade number index, t is time, $\vec{r}_B$ is the reference-blade ($m = 0$) complex displacement-amplitude vector, ω and σ are the temporal frequency and interblade phase angle, respectively, of the unsteady excitation and $Re\{\ \}$ denotes the real part of $\{\ \}$. Also, $p_{I,\mp\infty}$ and $\vec{\kappa}_{\mp\infty}$ are the amplitude and wave number, respectively, of an incident pressure fluctuation, $\tilde{p}_I(\vec{X}, t)$, coming from far upstream ($-\infty$) or far downstream ($+\infty$). Note that the interblade phase angle, σ, of an incident disturbance is $\vec{\kappa}_{\mp\infty} \cdot \vec{G}$. The temporal frequency and wave number of an incident vortical or entropic disturbance are related by $\omega = -\vec{\kappa}_{\mp\infty} \cdot \vec{G}$, but a more complicated relationship exists between ω and $\vec{\kappa}_{\mp\infty}$ for an incident pressure disturbance.

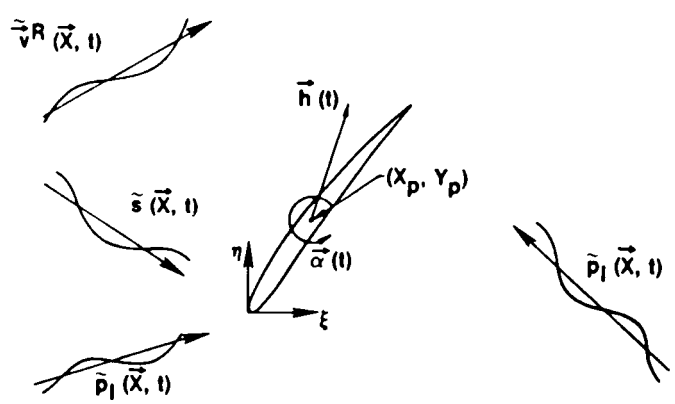

Blade motions: $\vec{\mathcal{R}}(\vec{X} + m\vec{G}, t) = \mathrm{Re}\left\{\vec{r}(\vec{X}) \exp\left[i\,(\omega t + m\sigma)\right]\right\}$

Incident disturbances: $\tilde{p}_{\mp\infty}(\vec{X}, t) = \mathrm{Re}\left\{p_{\mp\infty} \exp\left[i\,(\vec{\kappa}_{\mp\infty} \bullet \vec{X} + \omega t)\right]\right\}$

TIME-DEPENDENT GOVERNING EQUATIONS

The equations governing the fluid motion follow from the integral forms of the mass, momentum and energy conservation laws and the thermodynamic relations for a perfect gas. The former provide a coupled set of corresponding nonlinear differential equations (the Euler equations) in continuous regions of the flow and jump conditions at surfaces across which the inviscid flow variables are discontinuous, i.e., at vortex-sheet wakes and shocks. In continuous regions the energy equation can be replaced by the requirement that the entropy following a fluid particle must remain constant. In addition to the foregoing field equations and jump conditions, the attached flow assumption requires that the unsteady flow must be tangential to the moving blade surfaces and information on the uniform inlet and exit flow conditions and the incident entropic, vortical and acoustic or static pressure disturbances must be specified. The remaining steady and unsteady departures from the uniform inlet and exit conditions must be determined as part of the time-dependent solution. This foregoing aerodynamic problem is a formidable one as it involves a system of nonlinear time-dependent equations with conditions imposed on moving blade, wake and shock surfaces in which the instantaneous positions of the wakes and shocks must be determined as part of the solution. Because of these features and the prohibitive expense that would be involved in obtaining the aerodynamic response information needed for aeroelastic or aeroacoustic applications, the usual approach is to examine limiting forms of the full governing equations with the intention of providing efficient analyses for design applications.

- **Integral conservation laws**
- **Thermodynamic relations**

➡

- **Euler equations at field points**
- **Jump conditions at moving shocks ($\tilde{M}_f \neq 0$) and at vortex sheet boundary layers and wakes ($\tilde{M}_f = 0$)**
- **Flow tangency condition at moving blade surfaces**

- **Far-field behavior**

UNSTEADY AERODYNAMIC LINEARIZATIONS

Because of the complexity of the nonlinear time-dependent unsteady aerodynamic problem, linearized treatments of the unsteady flow are often considered. The major linearizations that have been proposed are the following: classical linearized theory, time-linearized transonic flow theory and the present theory in which unsteady disturbances are regarded as small relative to a fully nonuniform mean flow. The essential differences between these theories arise from the manner in which the steady flow is represented. In classical theory both steady and unsteady departures from a uniform stream are regarded as small and of the same order of magnitude. In time-linearized transonic theory steady and unsteady disturbances are regarded as small and very small, respectively, relative to uniform free-stream flow properties. Finally, in the present linearization no restriction is placed on the steady flow but the unsteady perturbations are assumed to be of small amplitude. The classical theory applies at the (reduced) frequencies of interest for turbomachinery applications, but steady flow variations have no impact on the unsteady response. Time-linearized transonic theory applies at Mach numbers near one and the unsteady perturbation depends on the steady flow, but this theory is formally restricted to low-frequency unsteady motions. The present theory fully includes the effects of nonuniform mean flow and applies throughout the Mach number and frequency range of interest for turbomachinery applications.

- **Classical theory**

$$\tilde{P}(x,y,t) = P_{-\infty} + \bar{p}(x,y) + \mathrm{Re}\left\{p(x,y)e^{i\omega t}\right\} + \ldots$$

- **Time-linearized transonic theory**

$$\tilde{P}(x,y,t) = P_{-\infty} + \bar{p}(x,\hat{y}) + \mathrm{Re}\left\{p(x,\hat{y})e^{i\omega t}\right\} + \ldots$$

- **Present theory**

$$\tilde{P}(x,y,t) = P(x,y) + \mathrm{Re}\left\{p(x,y)e^{i\omega t}\right\} + \ldots$$

PRESENT LINEARIZATION

The equations governing small-amplitude unsteady departures from a nonuniform mean flow are determined by expanding the various flow variables in asymptotic series in ϵ, where ϵ is a measure of the amplitude of the unsteady excitation. Thus, for example, in the first equation below $\tilde{P}(\vec{X},t)$ is the time-dependent fluid pressure, $P(\vec{X})$ is the pressure in the steady background flow, $Re\{p(\vec{X})e^{i\omega t}\}$ is the first-order time-dependent pressure and $p(\vec{X})$ is its complex amplitude. In addition, Taylor series expansions and surface vector relations are used to refer information at a moving blade, wake or shock surface ($\mathcal{S}$) to the mean position of this surface (S). Equations governing the zeroth-order or steady and the complex amplitudes of the first-order unsteady flow properties are obtained after substituting the foregoing expansions into the full time-dependent governing equations, equating terms of like power in ϵ and neglecting terms of higher than first order in ϵ. It follows from the original assumptions that the steady background flow is governed by a full-potential boundary-value problem and that the complex amplitudes of the unsteady flow properties are governed by a system of time-independent linearized equations with variable coefficients which depend on the underlying mean flow. In the unsteady problem surface conditions can be imposed at the mean surface locations, and in both the steady and first-order unsteady problems the required solution domain can be limited to a single extended blade-passage region.

- **Series expansions**

$$\tilde{P}(\vec{X},t) = P(\vec{X}) + Re\left\{p(\vec{X})e^{i\omega t}\right\} + \ldots$$

$$\tilde{P}_{\mathcal{S}} = (\tilde{P} + \vec{R}\cdot\nabla\tilde{P} + \ldots)_S$$

$$\vec{\tau}_{\mathcal{S}} = f(\vec{\tau}_S, \vec{R}) + \ldots.$$

$\Longrightarrow$

- **Full potential boundary-value problem for steady background flow**
- **Linear variable-coefficient boundary-value problem for first-order unsteady flow**
  - **Time-independent**
  - **Surface conditions at mean surface locations**
  - **Single extended blade-passage solution domain**

THE STEADY BACKGROUND FLOW

As a consequence of our assumptions regarding shocks and the steady flow far upstream of the blade row, the mean or steady background flow through the cascade will be homentropic and irrotational; i.e., $\vec{V} = \nabla\Phi$, where $\vec{V}$ and Φ are the local steady velocity and velocity potential, respectively. The field equations governing the steady flow follow from the mass and momentum conservation laws and the isentropic relations for a perfect gas. Here, $\bar{\rho}$, P, M and A and are the local steady density, pressure, Mach number and speed of sound propagation, respectively, and γ is the specific heat ratio of the fluid. Surface conditions for the zeroth-order or steady flow apply at the mean positions of the blade (B), wake (W) and Shock (Sh) surfaces. Blade mean positions are prescribed, but the mean wake, i.e., the stagnation streamlines downstream of the blade row, and shock positions must be determined as part of the steady solution. Since, by assumption, the flow remains attached to the blades, a flow tangency condition applies at blade surfaces. In addition the steady pressure and normal velocity component must be continuous across blade wakes and mass and tangential momentum must be conserved at shocks. Finally, three of the far-field uniform velocity components, or the equivalent information, must be prescribed to completely specify the steady boundary-value problem. The fourth or remaining component can be determined in terms of the three prescribed using the integral form of the mass conservation law.

- **Field equations** : $\nabla\cdot(\bar{\rho}\nabla\Phi) = 0$

$$\bar{\rho}^{(\gamma-1)} = \left(\gamma M_{-\infty}^2 P/2\right)^{(\gamma-1)/\gamma} = (M_{-\infty}A)^2 = F(\nabla\Phi)$$

- **Surface conditions**
  - **Blades** (B): $\nabla\Phi\cdot\vec{n} = 0$
  - **Wakes** (W): $[\![\nabla\Phi]\!]\cdot\vec{n} = 0,\ [\![\Phi]\!] = \text{constant}$
  - **Shocks** (Sh): $[\![\bar{\rho}\nabla\Phi]\!]\cdot\vec{n} = [\![\Phi]\!] = 0$
- **Far-field conditions**
  - **Uniform flow conditions**
  - **Analytic solutions for steady disturbances**

THE LINEARIZED UNSTEADY FLOW – 1

The field equations governing the first-order unsteady perturbation of a nonlinear homentropic and irrotational steady flow are determined from the full time-dependent mass, momentum and entropy transport equations and the thermodynamic equation relating the entropy, pressure and density of a perfect gas. These equations can be cast in a convenient form by introducing the Goldstein (ref. 2) velocity decomposition, i.e., $\vec{V} = \vec{v}^R + \nabla\phi$. The rotational component of the unsteady velocity ($\vec{v}^R$) is divergence-free far upstream of the blade row and it is independent of the pressure fluctuation (p); the irrotational component ($\nabla\phi$) is related directly to the unsteady pressure fluctuation. The resulting field equations for the first-order entropy (s), rotational velocity ($\vec{v}^R$) and velocity potential (ϕ) are given below. First-order partial differential equations describe the transport of entropy and rotational velocity through the blade row. The unsteady potential is governed by a second-order equation, which is locally elliptic at field points at which the local steady Mach number (M) is less than one and locally hyperbolic at those points at which $M > 1$. Note that the rotational velocity provides a forcing function term to the potential equation. Also, if there are no entropy and rotational velocity fluctuations at inlet, then only a single field equation must be solved to determine the unsteady flow.

- **Velocity decomposition** : $\vec{v} = \vec{v}^R + \nabla\phi$

  where $\vec{v}^R = f(s_{-\infty}, \vec{v}^R_{-\infty}, \nabla\Phi)$ **and** $p = -\bar{\rho}\,\dfrac{\bar{D}\phi}{Dt}$

- **Field equations**

$$\frac{\bar{D}s}{Dt} = 0$$

$$\frac{\bar{D}}{Dt}\left(\vec{v}^R - s\nabla\Phi/2\right) + \left[\left(\vec{v}^R - s\nabla\Phi/2\right)\cdot\nabla\right]\nabla\Phi = 0$$

$$\frac{\bar{D}}{Dt}\left(A^{-2}\frac{\bar{D}\phi}{Dt}\right) - \bar{\rho}^{-1}\nabla\cdot\left(\bar{\rho}\nabla\phi\right) = \bar{\rho}^{-1}\nabla\cdot\left(\bar{\rho}\vec{v}^R\right)$$

THE LINEARIZED UNSTEADY FLOW - 2

Conditions on the linearized unsteady perturbation at Blade (B), wake (W) and shock (Sh) mean positions are obtained in a similar fashion, i.e., by substituting the asymptotic, Taylor and surface-vector series expansions into the full time-dependent surface conditions and equating terms of like order in ϵ. The resulting first-order flow tangency, wake-jump (continuity of normal velocity and pressure) and shock-jump (conservation of mass and tangential momentum) conditions are indicated schematically below. Note that the blade displacement ($\vec{r}_B$) is prescribed but that the normal(to the shock) component of the shock displacement ($\vec{r}_{\mathrm{Sh}} \cdot \vec{n}$) must be determined as part of the unsteady solution. Wake displacements have no impact on the linearized unsteady problem. In addition to the surface conditions, we require information on the unsteady flows far upstream and far downstream from the blade row. In these regions the linearized unsteady equations reduce to the constant coefficient equations of classical linearized theory, and analytic solutions for the velocity potential fluctuations (ϕ^P) due to acoustic response disturbances and the far-downstream potential fluctuations (ϕ^R) associated with the vortical or rotational velocity disturbances can be determined. These analytic far-field solutions can be matched to near-field numerical solutions, and they thereby serve to complete the specification of the linearized unsteady boundary-value problem (ref. 3).

- **Surface conditions**
  - **Blades:** $\phi_n = f(\Phi, \vec{r}_B, \vec{v}^R)$
  - **Wakes:** $[\![\phi_n + \vec{v}_n^R]\!] = [\![p]\!] = 0$
  - **Shocks:** $[\![F(\Phi)\phi + G(\Phi)\phi_n]\!] = f(\Phi, \vec{r}_{sh,n}, \vec{v}^R)$

    $\vec{r}_{sh,n} = -[\![\phi]\!] / [\![\Phi_n]\!], \; [\![s]\!] = [\![\vec{v}^R]\!] = 0$
- **Far – field conditions**

  $s_{-\infty}, \vec{v}_{-\infty}^R$ **Prescribed**

  $$\phi_{\mp\infty} = \underbrace{\phi_{IN}^P}_{\text{Prescribed}} + \phi_{OUT}^P + \phi^R$$

NUMERICAL SOLUTION DOMAIN

The foregoing steady and linearized unsteady boundary-value problems account for the effects of blade geometry, mean blade loading and transonic, including moving shock, phenomena on the unsteady fluctuations arising from small-amplitude harmonic excitations. The unsteady equations are linear, time-independent and contain variable coefficients which depend on a fully nonlinear homentropic and irrotational steady background flow. Numerical resolutions of the nonlinear steady and the linearized unsteady problems are required to determine the aerodynamic response information needed for aeroelastic and aeroacoustic applications. Because of the cascade geometry and the assumed form of the unsteady excitations (i.e., periodic in t and η), such resolutions are required only over a single extended blade-passage region. In addition, since analytic far-field unsteady solutions have been determined, the numerical solution domain can be restricted further to a single extended blade-passage region of finite extent in the axial direction as shown below.

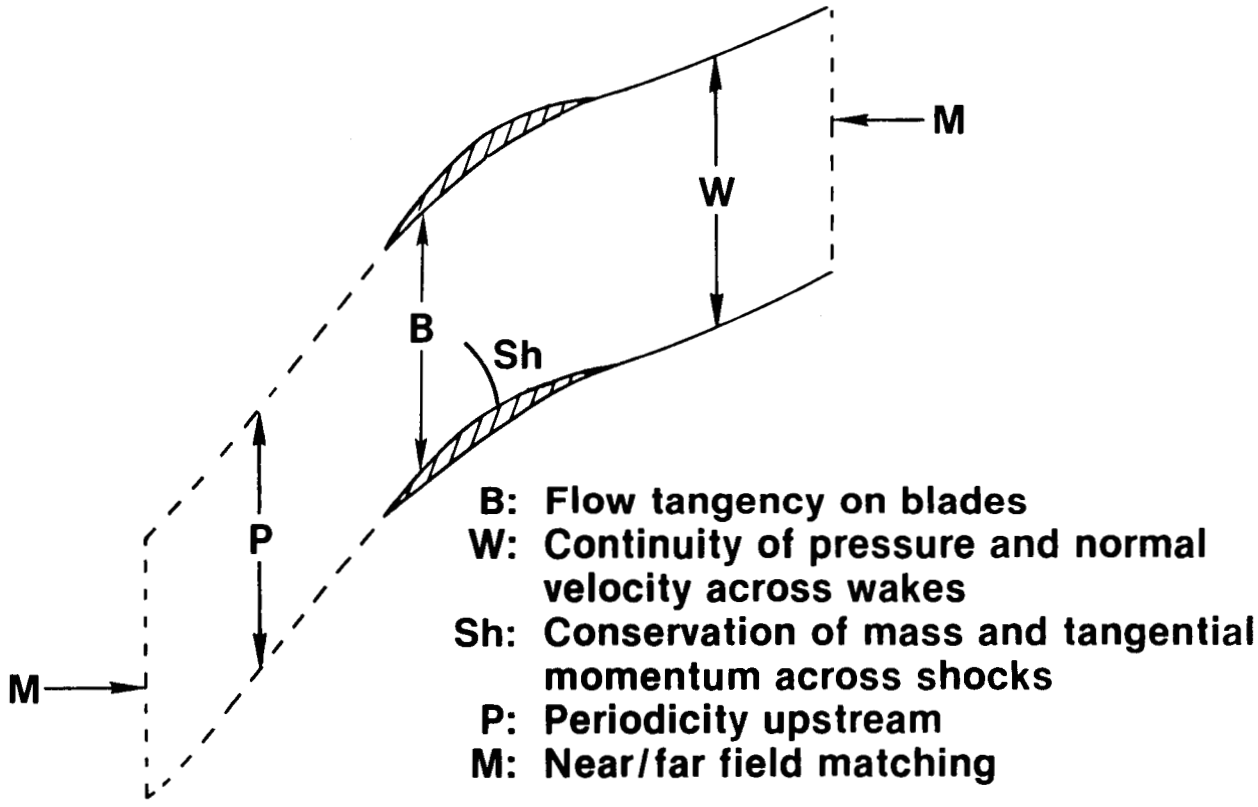

AERODYNAMIC RESPONSE AT A BLADE SURFACE

For aeroelastic and aeroacoustic applications, solutions to the nonlinear steady and the linearized unsteady boundary-value problems are required to predict the unsteady aerodynamic response at a moving blade surface (i.e., the unsteady surface pressures and the global unsteady airloads) and in the far-field (i.e., the unsteady pressure fluctuations), respectively. In particular, the pressure acting at the instantaneous position ($\mathcal{B}$) of a given blade surface is made up of two components: a harmonic component (p_H) which is determined by the steady (Φ) and the linearized unsteady (ϕ) potentials and the prescribed blade displacement ($\vec{r}_B$), and an anharmonic component (p_{Sh}) which is caused by the motion ($r_{\mathrm{Sh},B}$) of a shock along the blade surface. The anharmonic pressure is determined by analytically continuing the solution to the steady boundary-value problem from the mean to the instantaneous shock location (ref. 4). Although the pressure disturbance p_B is not everywhere harmonic, its regions of an harmonicity are small. Consequently, the first order global unsteady airloads are harmonic in time (ref. 5). In particular, if each two-dimensional blade section undergoes a pitching oscillation ($\vec{r}_B = \vec{\alpha} \times \vec{R}_p$) about an axis fixed to the blade, the first-harmonic unsteady moment is determined by integrating the product of the first-harmonic component of the unsteady surface pressure and $\vec{R}_p \cdot \vec{\tau}$ over the mean blade surface and subtracting a term consisting of the product of the steady pressure jump across the shock, $\vec{R}_p \cdot \vec{\tau}$ and the shock displacement along the blade surface.

Surface pressure

$$p_{\mathcal{B}} = p_H(\Phi, \phi, \vec{r}_B) + p_{Sh}(\Phi, r_{Sh,B}, t) + \ldots$$

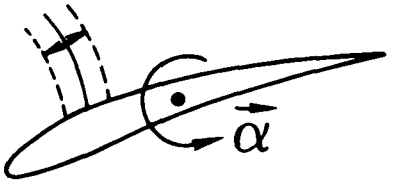

Unsteady moment

$$m = \oint p_H \vec{R}_p \bullet d\vec{\tau} - r_{Sh,B} [\![P_B]\!] (\vec{R}_p \bullet \vec{\tau})\Big|_B + \ldots$$

NUMERICAL RESULTS

At this point we have completed our description of the unsteady aerodynamic model and proceed to present numerical results to partially illustrate the status of numerical procedures for solving the nonlinear steady and linearized unsteady boundary-value problems and to demonstrate several important effects associated with nonuniform steady flow on the aerodynamic response at a moving blade surface. We refer the reader to refs. (6 and 7) for a description of the numerical procedures used. We will present results for two-dimensional compressor- or fan-type cascades operating at subsonic inlet and exit conditions. Theoretical results for steady surface Mach number (M) distributions, first-harmonic unsteady pressure-difference (Δp_H) distributions and unsteady aerodynamic moments (m) will be presented for blades undergoing pure pitching (torsional) motions with $\alpha = 1, 0$ about their midchords. The stability of such motions depends upon the sign of the out-of-phase moment (m_I). If $m_I > 0$, the airstream supplies energy to the blade motion, and this motion is unstable according to linearized theory. We will consider a subsonic cascade of NACA 0012 airfoils to illustrate the effects of a relatively thick, blunt-nosed blade geometry and variable mean incidence on the unsteady response and a subsonic/transonic cascade of 5% thick flat-bottomed double-circular-arc (DCA) airfoils to illustrate the effects of mean blade loading and transonic phenomena on the response at high subsonic inlet Mach number. For purposes of comparison results for flat-plate cascades, operating in uniform mean flows will be included along with those for the NACA 0012 and DCA cascades. The example cascades each have a stagger angle Θ of 45 deg and a unit gap/chord ratio ($G = 1$). The steady flows through the NACA 0012 and DCA cascades have been determined by imposing a zero-load condition at sharp blade edges.

- **Torsional vibrations about midchord: $r_B = (\vec{\alpha} \times \vec{R}_p)$**
- **Response parameters: Δp_H and m**
- **Subsonic flow: NACA 0012 airfoils**
- **Subsonic/transonic flow: DCA airfoils**

SUBSONIC FLOW: EFFECT OF INCIDENCE - 1

Steady and unsteady flows through the staggered cascade of modified NACA 0012 airfoils have been determined for an inlet Mach number ($M_{-\infty}$) of 0.6 and four inlet flow angles. The predicted surface Mach number distributions for $\Omega_{-\infty} = 48, 50, 52$ and 54 deg are shown below. The calculated exit Mach numbers are respectively 0.595, 0.557, 0.522 and 0.490, and in each case the calculated exit flow angle is approximately 47.7 deg. These steady flows are entirely subsonic with a peak Mach number of 0.789 occurring at $x = 0.113$ on the pressure (lower) surface of the blade for $\Omega_{-\infty} = 48$ deg, and 0.8, 0.86 and 0.96 occurring at $x = 0.07$, 0.05 and 0.03 on the suction (upper) surface for $\Omega_{-\infty} = 50$, 52 and 54 deg, respectively. In each case the mean flow stagnates within 0.2% of blade chord downstream from the leading edge.

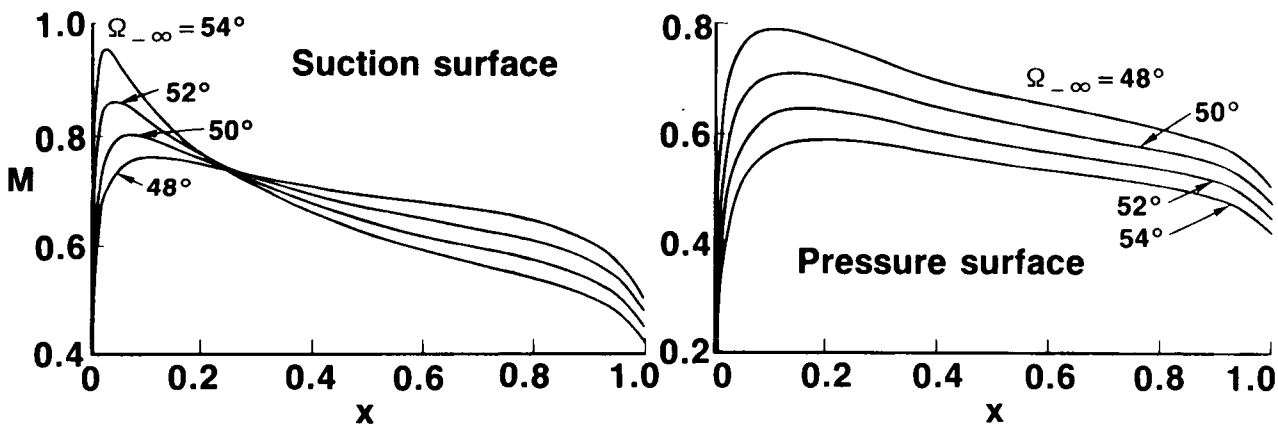

SUBSONIC FLOW: EFFECT OF INCIDENCE - 2

Unsteady response predictions for the NACA 0012 cascade and for a flat-plate cascade operating at $M_{-\infty} = 0.6$ and $\Omega_{-\infty} = 45°$ are shown on this and the next twofigures. Shown below are unsteady pressure-difference distributions and aerodynamic moments for the reference ($m = 0$) NACA 0012 and flat-plate blades undergoing unit-frequency pitching motions at $\sigma = 90$ deg. The unsteady pressure difference is singular and behaves like a multiple of $x^{-1/2}$ near the leading edge of the flat-plate airfoil. In contrast, the unsteady pressure is analytic in the vicinity of the rounded leading edge of the NACA 0012 blade. In this case both the real and imaginary components of the unsteady pressure difference are zero at the leading edge and reach local extrema very close to the leading edge. The results indicate that the coupling between the steady and unsteady flows, due to blade geometry and mean loading, leads to a reduction in the out-of-phase pressure difference, $Im\{\Delta p(x)\}$, over a forward part of the NACA 0012 blade and, therefore, a reduction in the out-of-phase moment opposing the blade motion.

Unsteady pressure difference distributions: NACA 0012 cascade; $\Theta = 45°$, $G = 1.0$, $M_{-\infty} = 0.6$, $\omega = 1.0$, $\sigma = 90°$.

____ NACA 0012 cascade, - - - - flat-plate cascade

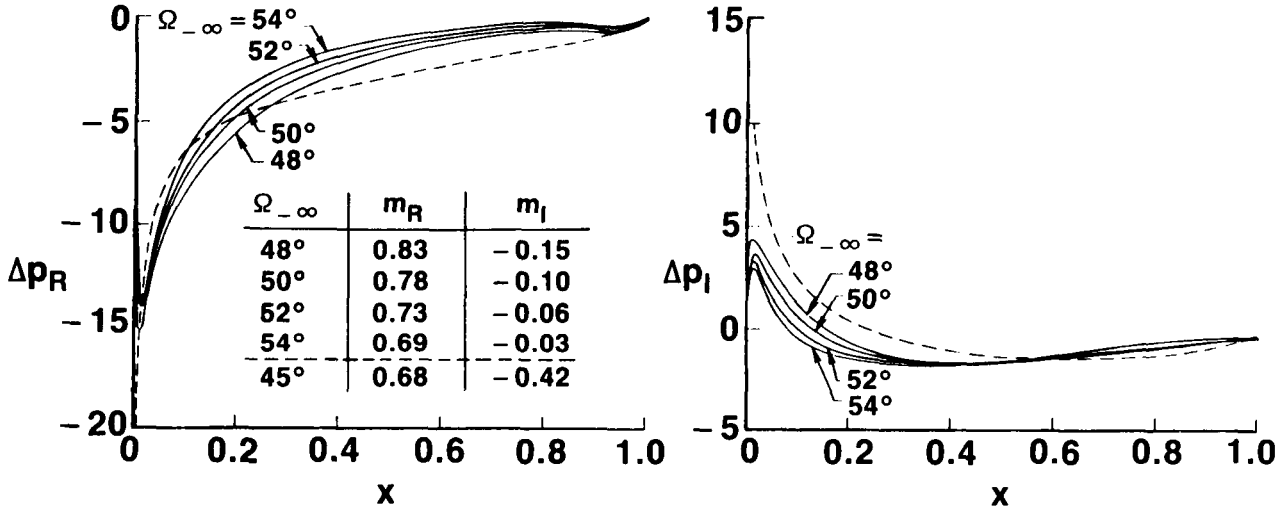

$\Omega_{-\infty}$	m_R	m_I
48°	0.83	-0.15
50°	0.78	-0.10
52°	0.73	-0.06
54°	0.69	-0.03
45°	0.68	-0.42

Unsteady moments acting on the reference blade of the NACA 0012 cascade operating at inlet flow angles of 48, 50, 52 and 54 deg and on the reference blade of the flat-plate cascade operating at $\Omega_{-\infty} = 45$ deg are shown below for blades undergoing unit-frequency torsional vibrations over the entire range of interblade phase angles, i.e., $\sigma \epsilon [-\pi, \pi]$. The abrupt changes in the moment curves are indicative of an acoustic resonance. The blade motions are superresonant (i.e., acoustic response disturbances persist in the far field and carry energy away from the blade row) at interblade phase angles lying between the lowest and highest resonant phase angles and subresonant (acoustic response disturbances attenuate with increasing distance from the blade row) at the interblade phase angles below the lowest and above the highest resonant phase angles. The blade motions considered below are stable but the NACA 0012 results indicate that the effect of mean blade loading tends to be destabilizing. Note that for a given σ the out-of-phase moment moves closer to the stability boundary as the inlet flow angle is increased.

Unsteady moment vs. interblade phase angle: $\Theta = 45°$, $G = 1.0$, $M_{-\infty} = 0.6$.

—— NACA 0012 cascade, – – – flat-plate cascade

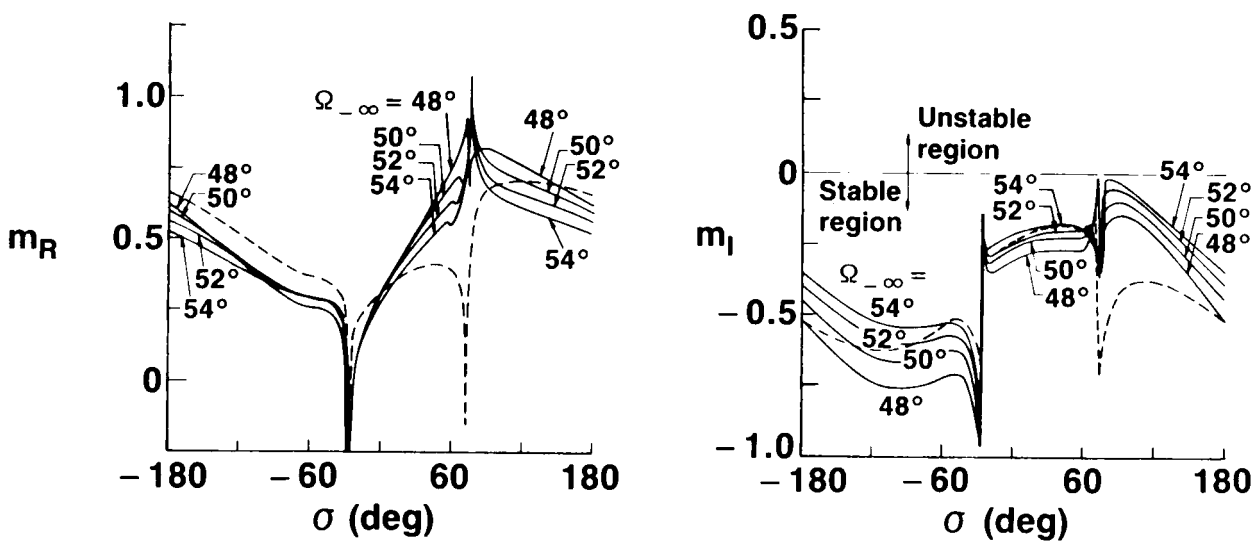

SUBSONIC FLOW: EFFECT OF FREQUENCY

The effect of frequency on the out-of-phase component of the unsteady moment due to torsion about midchord is illustrated below for the NACA 0012 cascade operating at $\Omega_{-\infty} = 54$ deg and for the flat-plate cascade operating at $\Omega_{-\infty} = 45$ deg. The NACA 0012 blades experience a region of subresonant torsional instability for $\omega = 0.25$, 0.5 and 0.75, with the extent of this region decreasing with increasing frequency. The subresonant torsional motions of the flat-plate cascade are unstable only at the lowest frequency considered, i.e., $\omega = 0.25$. Thus the nonuniform flow through the NACA 0012 cascade extends the frequency range over which the blades are susceptible to a torsional instability.

Unsteady moment vs. interblade phase angle:
$\Theta = 45°$, $G = 1.0$, $M_{-\infty} = 0.6$.

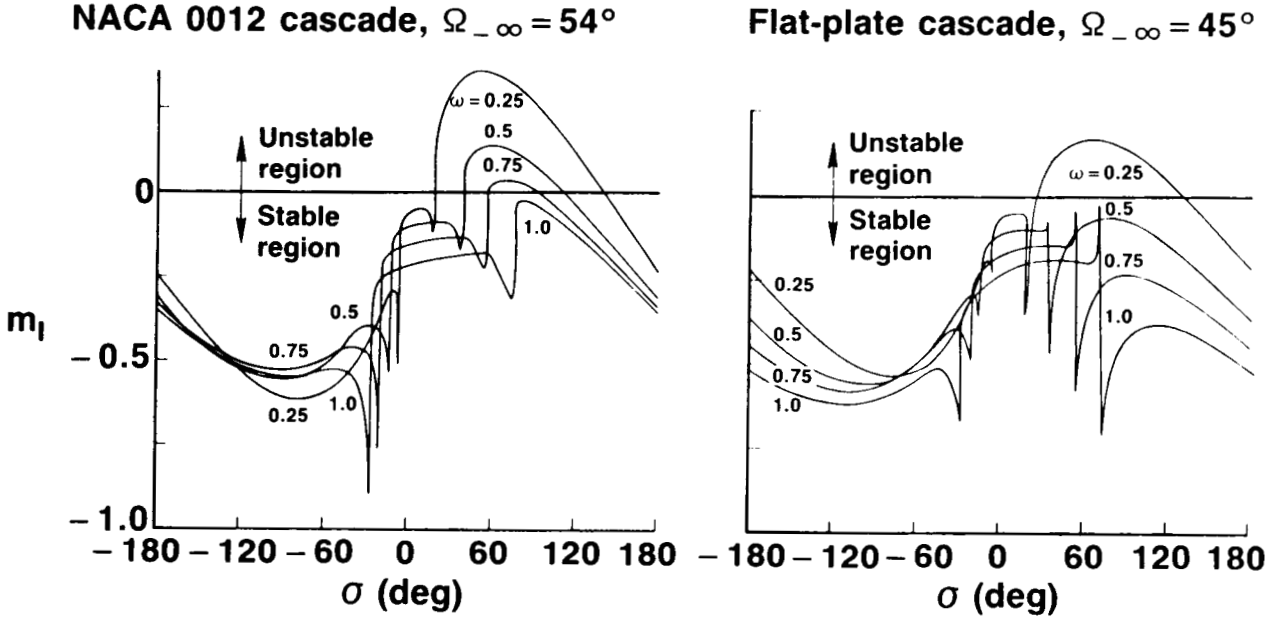

We now consider the staggered cascade of sharp-edged double-circular-arc airfoils. In particular, the airfoils have flat lower surfaces, circular arc upper surfaces and maximum thicknesses at midchord of 0.05. Full-potential steady and linearized unsteady flows through this example configuration have been determined for inlet Mach numbers of 0.5, 0.7, 0.8 and 0.9. The steady flows have been determined by imposing a zero-load requirement at blade leading and trailing edges. As a consequence, only the inlet Mach number is prescribed with the remaining inlet and exit parameters determined as part of the steady flow solution. Numerical results for this configuration along with those for a corresponding flat-plate cascade ($\Omega = 45$ deg, $G = 1$) are given in this and in the following three figures. Shown below are the predicted surface Mach number distributions for the example DCA cascade. For the prescribed inlet Mach numbers stated above, the calculated exit Mach numbers are 0.43, 0.57, 0.62 and 0.64, respectively. In addition, the calculated inlet flow angles are 49.0, 49.2, 49.4, and 49.6 deg, respectively, and in each case the calculated exit flow angle is approximately 43.0 deg. The steady flows at $M_{-\infty} = 0.5$, $M_{-\infty} = 0.7$ and $M_{-\infty} = 0.8$ are entirely subsonic with the maximum suction-surface Mach numbers of 0.561, 0.804 and 0.941 occurring at, respectively, 40.8, 38.5 and 36.5% of blade chord downstream from the leading edge. The steady flow at $M_{-\infty} = 0.9$ is transonic with the supersonic region extending from 18.5 to 52.5% of blade chord along the suction surface and terminating at a shock discontinuity. The Mach numbers at the foot of the shock are 1.193 on the upstream or supersonic side and 0.871 on the downstream or subsonic side.

Surface Mach number distributions: DCA cascade; $\Theta = 45°$, $G = 1.0$

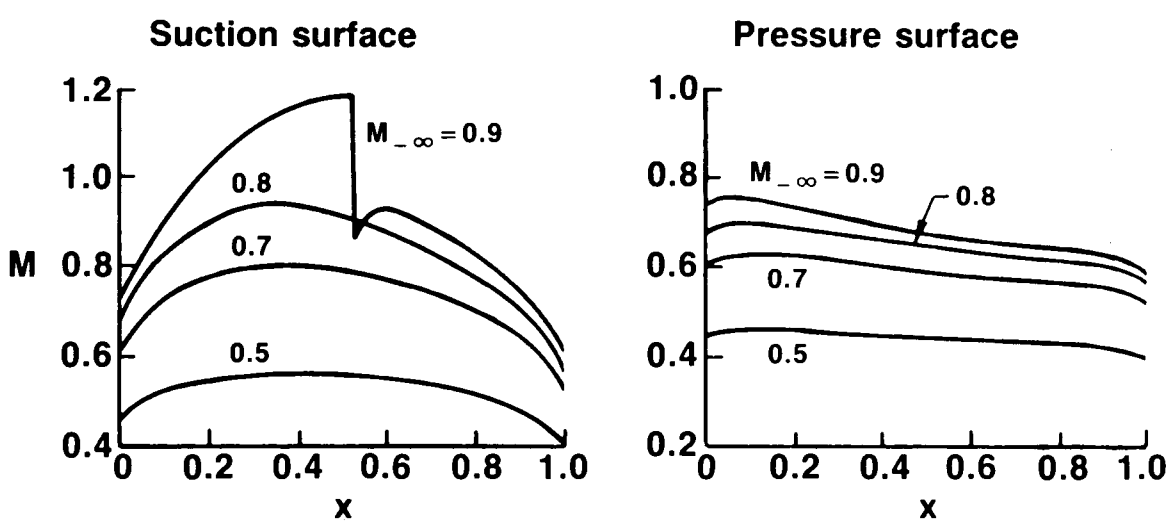

The effect of Mach number on the response to in-phase ($\sigma = 0$ deg) unit-frequency torsional blade vibrations is illustrated below for the DCA and flat-plate cascades. The blade motions at $\sigma = 0$ deg are superresonant. For the flows at $M_{-\infty} = 0.5$, 0.7 and 0.8 two acoustic waves persist in the far field—one upstream and one downstream—and propagate away from the blade row. For the DCA cascade operating at $M_{-\infty} = 0.9$ there are three such waves—two upstream and one downstream. Finally, for the flat-plate cascade operating at $M_{-\infty} = 0.9$ there are four such waves—two upstream and two downstream. The out-of-phase pressure-difference distributions and unsteady moments for the reference DCA and flat-plate blades reflect this change in character of the acoustic response in the far field, since the trends indicated by the results for $M_{-\infty} = 0.5$, 0.7 and 0.8 are not sustained at $M_{-\infty} = 0.9$. Also, a comparison of the DCA and flat-plate pressure-difference curves for in-phase motions suggests that the influence of mean flow gradients on the unsteady aerodynamic response becomes more pronounced with increasing Mach number. The pressure difference distributions for the DCA and flat-plate blades are very similar for the two lower inlet Mach number, differ somewhat for $M_{-\infty} = 0.8$ and differ substantially for $M_{-\infty} = 0.9$. The differences at $M_{-\infty} = 0.8$ can be attributed to the relatively large gradients in the subsonic mean flow that occur along the suction surface of each DCA blade. The substantial differences at $M_{-\infty} = 0.9$ are caused by the transonic effects associated with the DCA cascade and by the different far-field acoustic response environments produced by the two cascades.

Unsteady pressure-difference distributions and unsteady moments:
$\Theta = 45°$, $G = 1.0$, $\omega = 1.0$, $\sigma = 0°$.

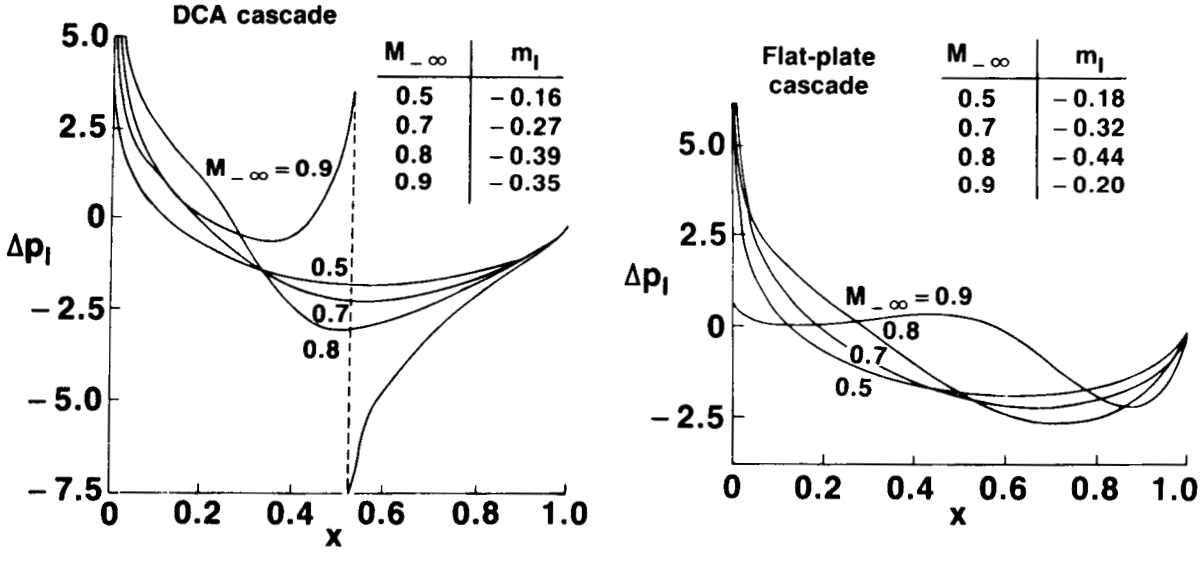

SUBSONIC/TRANSONIC FLOW: EFFECT OF FREQUENCY

Shown below are first-harmonic, out-of-phase, pressure-difference distributions and aerodynamic moments for the example DCA and flat-plate cascades operating at an inlet Mach number of 0.9. Here the blades are undergoing out-of-phase (σ = 180 deg) torsional vibrations about midchord at different prescribed frequencies. Recall that for a discontinuous transonic flow there are two contributions to the first-harmonic unsteady moment: one arising from the harmonic unsteady surface-pressure response and the other from the anharmonic surface pressures produced by shock motion. However, for the DCA cascade at $M_{-\infty} = 0.9$, the mean shock location is only slightly aft of blade midchord and, therefore, the anharmonic surface pressures make only a small contribution to the unsteady moment. A comparison of the DCA and flat-plate results depicted below indicates the dramatic impact of transonic mean-flow phenomena on unsteady aerodynamic response. A second interesting feature indicated by these results is the change in the unsteady moment behavior as the blade vibration frequency is increased from 0.25 to 0.5. This change occurs because the out-of-phase blade motions of the DCA and flat-plate cascades are subresonant for ω = 0.1 and 0.25 and superresonant for ω = 0.5, 0.75 and 1.0, and this change in the far-field acoustic response has an important impact on the unsteady aerodynamic response at a blade surface.

Unsteady pressure-difference distributions:
$\Theta = 45°$, $G = 1.0$, $M_{-\infty} = 0.9$, $\sigma = 180°$.

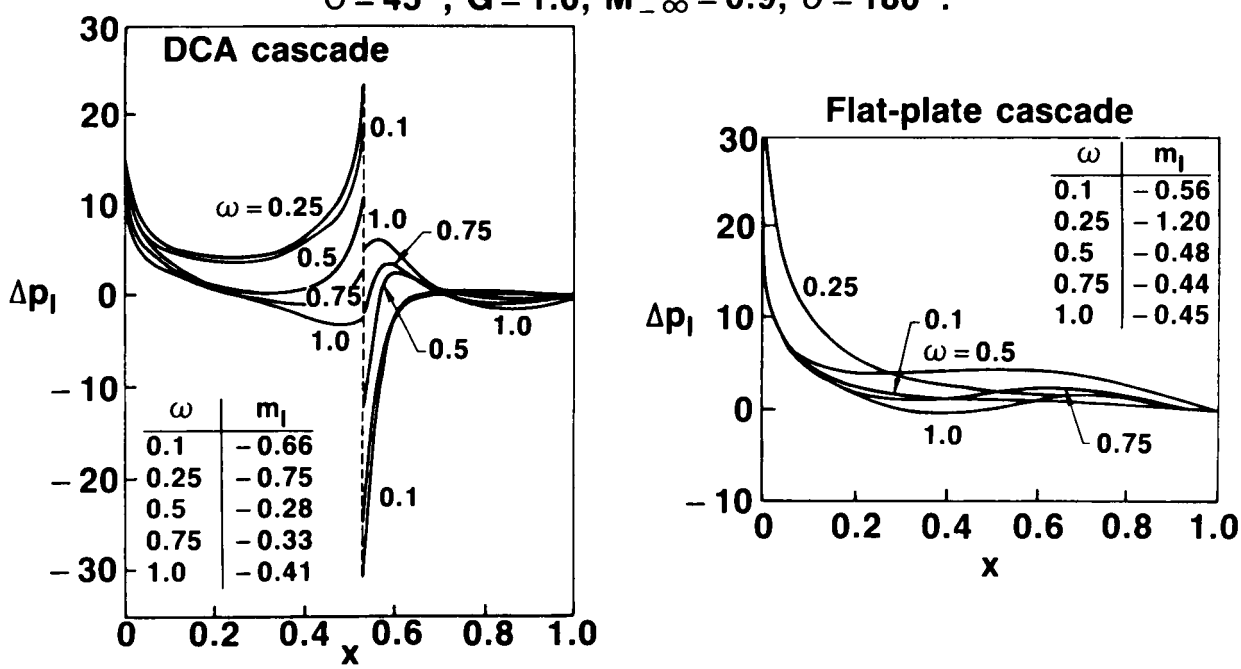

SUBSONIC/TRANSONIC FLOW

Finally, predictions of the aerodynamic moment versus interblade phase angle are shown for unit frequency torsional blade vibrations for the flat-plate and DCA cascades. Here $M_{-\infty} = 0.9$ and those angles at which an acoustic resonance occurs are indicated by the arrows at the top of each figure. The unit-frequency torsional blade motions of the two cascades are stable (i.e., $m_I < 0$ for all σ), but the behaviors of the flat-plate and DCA moment responses vs. interblade phase angle are quite different. These differences occur not only because the mean flow through the flat-plate cascade is entirely subsonic while that through the DCA cascade is transonic with a shock discontinuity, but also because of the substantial difference between the exit Mach numbers for the flat-plate ($M_\infty = 0.9$) and the DCA ($M_\infty = 0.64$) cascades. This difference implies that the two cascades operate in very different far-downstream acoustic response environments over almost the entire range of interblade phase angles.

Unsteady moment vs. interblade phase angle; ----m_R, —m_I

$\Theta = 45°$, $G = 1$, $M_{-\infty} = 0.9$, $\omega = 1.0$.

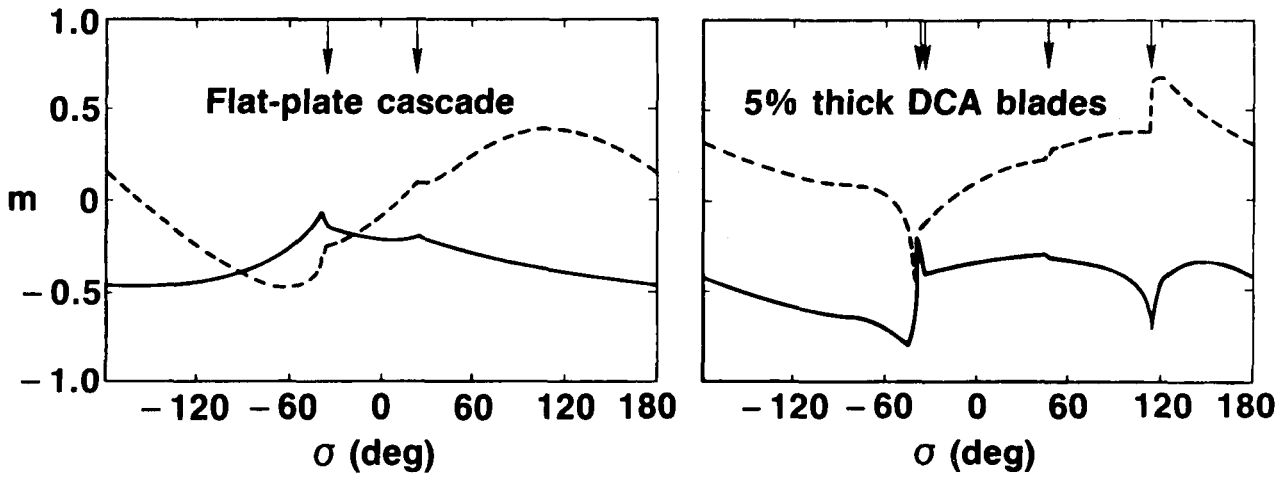

SUMMARY

The linearized unsteady aerodynamic theory outlined above accounts for the effects of real blade geometry, mean blade loading and operation at transonic Mach numbers on the unsteady aerodynamic response produced by the blades of an isolated two-dimensional cascade. This theory has been developed to meet the requirements of turbomachinery aeroelastic designers, but it should also be useful for aeroacoustic design applications. The unsteady flow is regarded as a small perturbation of a fully nonuniform isentropic and irrotational mean or steady flow, which is produced by small-amplitude temporally and spatially (in the cascade direction) periodic structural (blade motions) and external aerodynamic (incident entropic, vortical and acoustic disturbances) excitations. Thus the steady flow is determined as a solution of a full-potential boundary-value problem and the linearized unsteady flow as a solution of a time-independent, linear, variable-coefficient, boundary-value problem in which the variable coefficients depend on the underlying mean or steady flow.

Response predictions have been presented for the blades of compressor- and fan-type cascades undergoing pure torsional motions. In these examples there are no incident entropy or rotational velocity fluctuations and, therefore, only a single field equation must be solved to determine the linearized unsteady flow field. The numerical results demonstrate, to some extent, the status of numerical field methods for solving the nonlinear steady and the linear, variable-coefficient, unsteady, boundary-value problems and illustrate partially the effects of blade geometry, mean incidence, shock phenomena and differences between inlet and exit free-stream conditions on the unsteady response at blade surfaces.

- **Linearized unsteady aerodynamic analysis**
- **Effects of:**
  - **Blade geometry**
  - **Blade loading**
  - **Shocks and their motions**
  - **High frequency unsteady motions**
- **Blade flutter prediction**
- **Subsonic / transonic Mach numbers**

FUTURE DIRECTIONS

Linearizations relative to nonuniform steady flows offer great potential for meeting the needs of aeroelastic (or aeroacoustic) designers for efficient unsteady aerodynamic analyses that contain much of the essential physics associated with turbomachinery flow fields. However, before this potential can be fully realized, significant improvements in numerical solution methods for both the steady and linearized unsteady flows must be achieved so that reliable response information can be provided over the wide range of geometric configurations and flow conditions at which blade vibrations are of practical concern. In particular, unsteady aerodynamic analyses intended for turbomachinery aeroelastic predictions must be applicable to fan, compressor and turbine cascades, low subsonic through low supersonic Mach number operation and moderate through high frequency structural and external aerodynamic excitations. Some needed capabilities include the ability to predict transonic flows (i.e., subsonic flows with imbedded supersonic regions) through fan and compressor cascades operating at high positive or negative mean incidence, supersonic flows with complicated moving shock patterns and the high frequency unsteady flows caused by incident external aerodynamic disturbances. Major advances in our ability to predict turbomachinery aeroelastic and aeroacoustic behavior should result if future research is directed toward including the effects of strong viscid/inviscid interactions and possibly large-scale flow-separations within a linearized unsteady aerodynamic framework. Ultimately, linearized analyses which account for nonuniform steady flow and viscid/inviscid interaction phenomena must be extended to treat three-dimensional flows.

- **Subsonic/transonic flows at high incidence**

- **Forced aerodynamic excitations**

$$\mathcal{L}\phi = f(\vec{v}^R, s)$$

- **Supersonic Mach numbers**

- **Viscous separation phenomena**

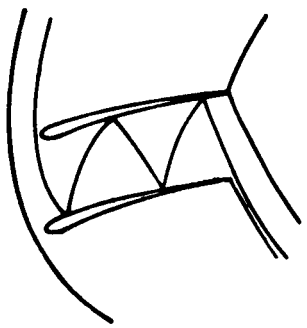

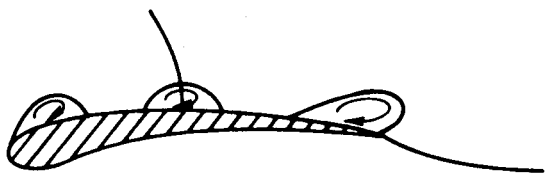

REFERENCES

1. Verdon, J. M. : Unsteady Aerodynamics of Blade Rows. In Proceedings of the Tenth U. S. National Congress of Applied Mechanics, J. P. Lamb (ed.), ASME, New York, January 1987, pp. 485-497.

2. Goldstein, M. E. : Unsteady Vortical and Entropic Distortions of Potential Flows Round Arbitrary Obstacles. Journal of Fluid Mechanics, vol. 89, part 3, 1978, pp. 433-468.

3. Verdon, J. M. : Linearized Unsteady Aerodynamic Theory. Chapter 2 in AGARD Manual on Aeroelasticity in Axial Flow Turbomachines, vol. I, M. F. Platzer and F. O. Carta (eds.), March 1987.

4. Williams, M. H. : Linearization of Unsteady Transonic Flows Containing Shocks. AIAA Journal, vol. 17, no. 4, April 1979, pp. 394-397.

5. Ehlers F. E. and Weatherill, W. H. : A Harmonic Analysis Method for Unsteady Transonic Flow and Its Application to the Flutter of Airfoils. NASA CR 3537, May 1982.

6. Caspar, J. R. : Unconditionally Stable Calculation of Transonic Potential Flow Through Cascades Using an Adaptive Mesh for Shock Capture. Trans. ASME A: Journal of Engineering for Power, vol. 105, no. 3, July 1983, pp. 504-513.

7. Verdon, J. M. and Caspar, J. R. : A Linearized Unsteady Aerodynamic Analysis for Transonic Cascades. Journal of Fluid Mechanics, vol. 149, December 1984, pp. 403-429.